Articles in PresS. Am J Physiol Lung Cell Mol Physiol (November 21, 2014). doi:10.1152/ajplung.00179.2014

Alpha-1-Antitrypsin Variants and the Proteinase/Anti-Proteinase Imbalance in Chronic Obstructive Pulmonary Disease

Nicola J Sinden[1*], Michael J Baker[2*], David J Smith[3], Jan-Ulrich Kreft[4,5,6], Timothy R Dafforn[5], Robert A Stockley[1].

[1]Centre for Translational Inflammation Research, University of Birmingham Research Laboratories, Queen Elizabeth Hospital, Birmingham, B15 2WB, United Kingdom.

[2]School of Life Sciences, University of Warwick, Coventry, CV4 7AL, United Kingdom.

[3]School of Mathematics, University of Birmingham, Birmingham B15 2TT, United Kingdom.

[4]Centre for Systems Biology, University of Birmingham, Birmingham, B15 2TT, United Kingdom.

[5]School of Biosciences, University of Birmingham, Birmingham B15 2TT, United Kingdom.

[6]Institute of Microbiology and Infection, University of Birmingham, Birmingham B15 2TT, United Kingdom.

[*]Joint first authors.

Correspondence to: Robert A. Stockley, Lung Function and Sleep Department, ADAPT Office (Office 4), Queen Elizabeth Hospital Birmingham, B15 2WB, UK.

E-mail: rob.stockley@uhb.nhs.uk; Telephone: +44 (0) 121 3713885; Fax: +44 (0) 121 3713887.

Running title: The proteinase/anti-proteinase imbalance in lung disease

Author contributions

NJS recruited patients, collected blood samples, co-designed and performed the laboratory experiments, assisted with interpreting the results and co-wrote the manuscript. MJB contributed to data analysis (enzyme kinetics), design of the mathematical model and co-wrote the manuscript. DS designed the mathematical model and numerical code, and edited the manuscript. JUK contributed to data analysis (enzyme kinetics), design of the mathematical model and edited the manuscript. TD contributed to data analysis (enzyme kinetics), design of the mathematical model and edited the manuscript. RAS co-designed the laboratory experiments, assisted with interpretation of results, developed the concept of mathematical modelling and edited the manuscript.

Abstract

The excessive activities of the serine proteinases neutrophil elastase and proteinase 3 are associated with tissue damage in chronic obstructive pulmonary disease. Reduced concentrations and/or inhibitory efficiency of the main circulating serine proteinase inhibitor alpha-1-antitrypsin result from point mutations in its gene. In addition, alpha-2-macroglobulin competes with alpha-1-antitrypsin for proteinases and the alpha-2-macroglobulin sequestered enzyme can retain its catalytic activity. We have studied how serine proteinases partition between these inhibitors and the effects of alpha-1-antitrypsin mutations on this partitioning. Subsequently, we have developed a three dimensional reaction-diffusion model to describe events occurring in the lung interstitium when serine proteinases diffuse from the neutrophil azurophil granule following degranulation, and subsequently bind to either alpha-1-antitrypsin or alpha-2-macroglobulin. We found that the proteinases remained uninhibited on the order of 0.1 s after release, and diffused on the order of 10 μm into the tissue before becoming sequestered. We have shown that proteinases sequestered to alpha-2-macroglobulin retain their proteolytic activity, and that neutrophil elastase complexes with alpha-2-macroglobulin are able to degrade elastin. Although neutrophil elastase is implicated in the pathophysiology of emphysema, our results highlight a potentially important role for proteinase 3 due to its greater concentration in azurophil granules, its reduced association rate constant with all alpha-1-antitrypsin variants studied here, its greater diffusion distance and time spent uninhibited following degranulation, and its greater propensity to partition to alpha-2-macroglobulin where it retains proteolytic activity.

Key words

Alpha-1-antitrypsin/ chronic obstructive pulmonary disease/ reaction-diffusion model/ enzyme kinetics/ serine proteinase

Abbreviations

A1AT	Alpha-1-antitrypsin
A1ATD	Alpha-1-antitrypsin deficiency
A2M	Alpha-2-Macroglobulin
ARDS	Adult respiratory distress syndrome
COPD	Chronic obstructive pulmonary disease
CT	Computed tomography
DMSO	Dimethyl sulfoxide
ELISA	Enzyme linked immunosorbent assay
FRET	Förster resonance energy transfer
K_{ass}	Second order association rate constant
K_{cat}	Catalytic constant
K_m	Michaelis constant
MSaapvN	N-Methoxysuccinyl-Ala-Ala-Pro-Val p-nitroanilide
NE	Neutrophil elastase
NSP	Neutrophil serine proteinase
PPE	Porcine pancreatic elastase
PR3	Proteinase 3
R_{max}	Maximum diffusion distance
SEM	Standard error of the mean
SlaaapN	N-succinyl-Ala-Ala-Ala-p-nitroanilide
SLPI	Secretory leukoproteinase inhibitor
T_{max}	Maximum time free in solution

Introduction

Chronic obstructive pulmonary disease (COPD) is a major cause of morbidity and mortality worldwide (40) and creates a significant economic burden (60). Several pulmonary phenotypes have been recognised, including chronic bronchitis which affects the large airways and is associated with chronic mucus hypersecretion (32), and emphysema which is associated with destruction of alveolar walls and enlargement of airspaces distal to the terminal bronchioles (38). Although the main risk factor for the development of COPD is cigarette smoking (10), only around 20% of smokers develop clinically significant disease (49) indicating that other environmental and genetic risk factors are important in the aetiology. To date, deficiency of the serine proteinase inhibitor (serpin) alpha-1-antitrypsin (A1AT) is the only widely recognised genetic predisposition.

A1AT is secreted by hepatocytes (16), enters the lungs primarily by passive diffusion and inhibits neutrophil serine proteinases (NSPs) irreversibly with 1:1 stoichiometry. Circulating levels of A1AT are in the range of 20-53 μM in individuals with the normal (PiMM) genotype (5). Over 100 naturally occurring genetic variants of A1AT have been described. The most common allele associated with marked deficiency of A1AT is the Z variant (glutamate 342→lysine) which is characterised by a reduction in A1AT quantity (approximately 20% of the serum level of the normal M variant), a reduction in inhibitory efficiency and a tendency to form polymers that are retained in the synthesising cell (24). Pathological consequences then result from a reduction in circulating levels of A1AT increasing the risk of developing early-onset emphysema (12), due to the reduced ability to control NSP activity in the tissues. Other variants described in this paper include the S (glutamate 264→valine), F (arginine 223→ cysteine) and I (arginine 39→cysteine) variants, which have also been identified in subjects with lung disease, although less commonly than

106 the Z variant (2, 15). Population and *in vitro* studies (7) suggest that below a minimum serum
107 A1AT threshold of 11 μM, A1AT is markedly less able to protect the lungs from NSPs,
108 leading to an increased risk of developing emphysema.
109
110 The NSP family includes neutrophil elastase (NE) and proteinase 3 (PR3) which have been
111 shown directly to cause pathological changes consistent with emphysema in animal models
112 (14, 26). Although many studies to date have focussed on the importance of NE in the
113 proteinase/anti-proteinase imbalance (45, 50), there is increasing evidence that other NSPs
114 such as PR3 may also play an important role (44). PR3 is the most abundant serine proteinase
115 in the neutrophil with each cell being estimated to store 3 and 1.1 pg of PR3 and NE
116 respectively (8). In addition, inhibition of PR3 in the lungs is likely to be less efficient than
117 for NE because PR3 is not inhibited by the locally produced chelonianin inhibitor, secretory
118 leukoproteinase inhibitor (SLPI) (4), and the remaining airway inhibitors A1AT and elafin
119 bind to NE more readily than to PR3 (59). The third NSP, cathepsin G, has not been shown to
120 produce emphysema-like lesions in animal or *in vitro* studies to date, and was therefore not
121 included in the current study.
122
123 Previous studies of the proteinase/anti-proteinase imbalance in COPD have not taken into
124 account factors such as; competitive binding when more than 1 NSP is released; when NSPs
125 are released in varying amounts; and differences in the association rate constants for each
126 NSP. Furthermore (at least in serum), a second inhibitor, alpha-2 macroglobulin (A2M) will
127 also compete with A1AT for NSPs and, at least for NE, the sequestered enzyme may retain
128 its catalytic activity (52). In this paper, we have studied how the NSPs NE and PR3 partition
129 between their inhibitors A1AT and A2M following degranulation, and the effects of A1AT
130 mutations on this partitioning. We have developed a three dimensional reaction-diffusion

131 model to describe events likely to occur in the lung interstitium and hence pertinent to the
132 pathophysiology of emphysema. The model describes the diffusion of NE and PR3 from an
133 azurophil granule following external degranulation, and their subsequent inhibition by
134 binding to either A2M or A1AT. The results highlight the importance of PR3 in the
135 proteinase/anti-proteinase imbalance in emphysema, and increase our understanding of the
136 mechanisms involved which may have implications for treatment of alpha-1-antitrypsin
137 deficiency (A1ATD) (including the role of A1AT augmentation therapy) and usual COPD.

Materials and methods

Subject selection

Subjects with A1ATD were identified from the U.K. national registry (based at Queen Elizabeth Hospital, Birmingham, U.K.) and had their diagnosis confirmed by phenotyping and genotyping (Heredilab, Salt Lake City, Utah, USA). Healthy controls were partners of patients with A1ATD and had a normal PiMM A1AT phenotype. All subjects provided written informed consent and ethical approval was obtained for all aspects of this study (South Birmingham Research Ethics Committee LREC 3359).

Sample collection

Venous blood was collected from all subjects and processed within 30 minutes of collection. Serum was obtained using Vacuette® serum tubes (Greiner bio-one, UK), allowing clot formation. The tubes were centrifuged at 1800 x g for ten minutes at room temperature, and serum was harvested and stored in multiple aliquots at -70 ºC until analysis, to minimise freeze-thaw cycles.

Active site titration of enzymes

Pure PR3 (Merck, Feltham, UK, EC number 3.4.21.76) and pure NE (Athens Research and Technology, Athens, GA, USA, EC number 3.4.21.37) were active site titrated against pure M variant A1AT (Athens Research and Technology), as described previously (44).

Measurement of A1AT and A2M concentrations in serum samples

The A1AT concentration was measured in the serum samples using a locally developed ELISA which has been described elsewhere (44). The A2M concentrations of serum samples

were determined using a commercially available A2M ELISA kit (Universal Biologicals Cambridge, UK), according to the manufacturer's instructions.

Inhibition assays of NSPs with serum from various A1AT genotypes

Pure NE of pre-determined activity was diluted in NE assay buffer (0.01 M Tris-HCl, 0.5 M NaCl, 0.1% Triton X100, pH 8.6) to 1.5 μM active enzyme. Serum samples from subjects with various A1AT genotypes were taken and the A1AT concentration was measured by ELISA. Each serum sample was then diluted in NE assay buffer so that the concentration of A1AT was 1.5 μM. Ten μL of NE was added to a 96-well plate (Costar, USA) in triplicate sets and increasing volumes of serum were then added to each set of wells. Each experimental set had an appropriate control containing no NE, but containing all other components including diluted serum. All wells were made up to 110 μL with NE assay buffer, and the plate was covered and incubated with gentle shaking at 37ºC for 20 minutes to allow the NE to form complexes with the serum inhibitors. Residual activity was measured by adding 100 μL of the NE specific substrate N-succinyl-Ala-Ala-Ala-p-nitroanilide (SlaaapN; Sigma-Aldrich, Gillingham, UK) at a concentration of 1 mg/ml in NE assay buffer. The absorbance at 410 nm was read at 5 minute intervals up to 60 minutes using a Biotek Synergy HT plate reader at 37ºC. Average results were taken for all triplicates and control values were subtracted. Inhibition slopes were constructed by plotting the percentage of remaining enzyme activity against the molar ratio of A1AT:NE, and each experiment was performed in triplicate.

NE inhibition assays were also performed using 150 μL of the substrate N-Methoxysuccinyl-Ala-Ala-Pro-Val p-nitroanilide (MSaapvN; Sigma-Aldrich) at a concentration of 0.2 mg/ml in NSP assay buffer (50 mM Hepes, pH 7.4, 150 mM NaCl, 0.05% Igepal CA-630 (v/v)). For

these experiments, NE was used at a lower concentration of 0.1 μM due to the different kinetic parameters between the substrates (57), and the serum samples were diluted accordingly.

PR3 inhibition assays were performed using a similar method with an active PR3 concentration of 1.5 μM and the serum samples diluted accordingly. These experiments were performed in NSP assay buffer, and used MSaapvN as the substrate, which is hydrolysed by both NE and PR3.

Inhibition of NSPs with mixtures of pure A2M and pure A1AT

Using the values obtained from the A2M and A1AT ELISAs for serum samples, mixtures of pure A2M and pure M variant A1AT were created in the same concentrations as would be found in the serum samples. Inhibition assays of NSP activity were then performed as described above.

Inhibition assays of NSPs using elastin-fluorescein as the substrate

Pure NE or PR3 were diluted in elastin buffer (0.2 M Tris base, pH 8.8) to an active concentration of 1.5 μM, and 20 μL was added to an eppendorf 1.5 ml tube (Eppendorf, UK). Serum or pure A1AT was diluted in elastin buffer so that the concentration of A1AT was 1.5 μM and increasing volumes of serum/A1AT were added to each eppendorf tube. The total volume in each tube was made up to 300 μL with elastin buffer and the tubes were incubated for 20 minutes at 37ºC to allow the NE or PR3 to form complexes with inhibitors. The control tube contained buffer alone. After incubation, 200 μL of elastin-fluorescein (Elastin products, USA, purified from bovine neck ligament and labelled with fluorescein-isothiocyanate) was added and the tubes were incubated on a blood tube rotator at 37ºC for

20 hours. The tubes were centrifuged and 100 µL of supernatant was taken and added to a 96-well plate and the absorbance was read at 495 nm in a Biotek Synergy HT plate reader. Control values were subtracted and inhibition slopes were constructed by plotting the percentage of remaining enzyme activity against the molar ratio of A1AT to NE or PR3.

Treatment of serum with methylamine to inactivate A2M

In order to measure the second order association rate constant (K_{ass}) values for serum A1AT with NE or PR3, it was first necessary to inactivate A2M. This was achieved by treating the serum samples with 0.1 M methylamine (Fisher Scientific, UK) for 10 minutes at 37°C (33). The inactivation of A2M was confirmed indirectly by measuring NE and PR3 inhibition by serum samples with and without treatment with methylamine. The substrate used for these experiments was MSaapvN at 0.6 mg/ml in 0.1 M Hepes, pH 7.5, 9.5% dimethyl sulfoxide (DMSO).

Measurement of K_{ass} for A1AT variants and NE

Pure NE of pre-determined activity was diluted to an active concentration of 100 nM with NSP assay buffer. Methylamine-treated serum samples of various A1AT genotypes were also diluted to an A1AT concentration of 100 nM, and these samples were titrated against NE to determine the percentage of active A1AT. Following this initial step, the time-dependent measurements were performed by incubating equimolar amounts of NE and active A1AT (1 nM each) in a 1 ml polystyrene cuvette with a 1 cm pathlength at 23°C. Residual NE activity at 1-5 minutes was measured by the addition of 200 µL of MSaapvN and measurement of the change in absorbance (410 nm) over 10 minutes using a spectrophotometer (Jasco V550). At each time point, the percentage of NE inhibition was determined. The K_{ass} was calculated by

plotting the inverse of NE activity at each time point versus time. From the linear portion of the slope, the half time ($t_{½}$) of the reaction was calculated using the formula;

$$t_{1/2} = c/m \quad (1)$$

Where c is the y-axis intercept and m is the gradient of the line.

K_{ass} was calculated using the equation (34);

$$K_{ass} = \frac{1}{[NSP] \times t_{1/2}} \quad (2)$$

Measurement of K_{ass} for A1AT variants and PR3

Pure PR3 of pre-determined activity was diluted to an active concentration of 400 nM with NSP assay buffer. Methylamine-treated serum samples were also diluted to an A1AT concentration of 400 nM and these samples were titrated against PR3 to determine the percentage of active A1AT. Following this initial step, the time-dependent measurements were performed by incubating equimolar amounts of PR3 and active A1AT (1 nM each) in a black opaque polypropylene low binding plate (Sigma, UK) at 23°C with a well volume of 150 µL. Residual PR3 activity at 1-5 minutes was measured by adding 3 µL of the PR3 specific Förster resonance energy transfer (FRET) substrate Abz-VAD-norV-ADRQ-EDDnp (Alta Biosciences, UK) at a concentration of 1 mM (18). The change in fluorescence (excitation 320 nm, emission 420 nm) was measured every 2 minutes for 20 minutes using a Biotek Synergy 2 Multi-Mode Microplate Reader. At each time point, the percentage of PR3 inhibition was determined. The K_{ass} was calculated using the same method as that used for NE.

261

262 Development of a three dimensional reaction-diffusion model

263 *Model parameters*

264 The diffusion of PR3 and NE from the azurophil granule following external degranulation
265 and their subsequent binding reactions with inhibitors was modelled by a system of
266 spherically symmetric reaction-diffusion equations and solved numerically by a finite
267 difference method implemented in the software MATLAB version R2013a 8.1.0
268 (MathWorks, MA, USA). Reactions between NSPs and inhibitors were treated as irreversible
269 mass action equations based on their respective K_{ass} values:

270

271 $$E + S \xrightarrow{K_{ass}} ES \quad (3)$$

272

273 Where E is the enzyme (NSP) and S is the inhibitor. Although dissociation of the complex to
274 form inactivated inhibitor may occur, the rate is not sufficient to significantly change the
275 stoichiometry of inhibition or the quantity of inactivated inhibitor (28). Therefore these
276 reactions based on K_{ass} values are valid approximations.

277

278 K_{ass} values or A1AT concentrations for PiMZ and PiSZ sera were not determined in this
279 study. However, we were able to model these variants by adjusting the model code such that
280 the two A1AT variants in these heterozygous states were treated as separate entities. We
281 assumed that 50% of the total A1AT concentrations in the PiMM, PiSS and PiZZ
282 homozygotes (see Table 1) contributed equivalent A1AT concentrations to PiMZ and PiSZ
283 heterozygotes, and that each A1AT variant had the same K_{ass} value as in the homozygote (see
284 Table 2). Therefore values of 15.15 μM for M A1AT, 7.2 μM for S A1AT and 2.15 μM for Z

A1AT were used, giving total A1AT concentrations of 17.3 μM for PiMZ and 9.35 μM for PiSZ.

Starting concentrations of PR3 and NE were taken as 13.4 mM (8) and 5.4 mM (22) respectively and confined to a volume approximating the azurophil granule with radius 0.171 μm and volume of 2.28 x 10^{-17} L, as published elsewhere (22). A1AT serum concentrations for each variant were calculated as described above, and an A2M concentration of 3 μM was used as published previously (6) and confirmed by measured values in this study. Association rate constants of A2M with NE and PR3 were given as 4.1 x 10^{7} $M^{-1}s^{-1}$ and 1.1 x 10^{7} $M^{-1}s^{-1}$ respectively as previously published (41, 54).

Reaction-diffusion equations

Reaction-diffusion of NSPs were modeled via partial differential equations, as

$$\frac{\partial[NE]}{\partial t} = D_{NE}\nabla^2[NE] - K_{A1AT:NE}[A1AT][NE] - K_{A2M:NE}[A2M][NE] \quad (4)$$

with an analogous equation holding for [PR3].

The three-dimensional spherically symmetric Laplacian operator is given by,

$$\nabla^2 = r^{-2}\partial_r(r^2\partial_r). \quad (5)$$

The diffusion coefficients (*D*) for PR3, NE, A1AT and A2M were estimated as 7.94, 7.90, 6.54 and 2.72×10^{-11} m^2s^{-1} respectively as per equation 6 from Tyn and Gusek (53) $D = 2.44\times10^{-9}\ m^2\ s^{-1}\ g^{1/3}\ mol^{-1/3} \times M^{-1/3}$, where *M* is the molecular mass in g mol^{-1}. Diffusivity decreases with molecular mass, but not much since *D* decreases with the inverse of the radius and therefore with the inverse of the cube root of molecular mass. Inhibitors were assumed to

be present long before the release of the NSPs and hence spatially uniformly distributed initially. Reaction-diffusion of inhibitors was modelled by

$$\frac{\partial[A1AT]}{\partial t} = D_{A1AT}\nabla^2[A1AT] - K_{A1AT:NE}[A1AT][NE] - K_{A1AT:PR3}[A1AT][PR3], \quad (6)$$

with an analogous equation holding for [A2M].

Finally, NSP-inhibitor complexes were also assumed to diffuse, approximately at the same rate as free inhibitor, and therefore evolve as

$$\frac{\partial[A1AT:NE]}{\partial t} = D_{A1AT}\nabla^2[A1AT:NE] + K_{A1AT:NE}[A1AT][NE], \quad (7)$$

with analogous equations holding for [A2M:NE], [A1AT:PR3] and [A2M:PR3].

The system was solved on the domain 0.02 μm < r < 50 μm for a time period of 0 < t < 0.5 s, with no-flux (zero-derivative) boundary conditions at r = 0, 50 μm, the domain being chosen sufficiently large that the choice of condition at the outer boundary does not significantly affect the results. Initial conditions were taken as spatially uniform for inhibitor, zero for complex, and a smoothed step function of radius 0.171 μm for enzyme boluses.

The equations were solved numerically via the Crank-Nicholson method (31) for the diffusion operator, and first order forward time difference for nonlinear reaction terms. The spatial and temporal discretisations of δr = 0.01 μm and δt = 0.4 μs were verified to be sufficiently small by testing the results against those calculated with finer spatial and temporal grids.

Calculation of R_{max}, T_{max} and partitioning

Maximum diffusion distances (R_{max}) and maximum time free in solution (T_{max}) were calculated from the resultant matrices generated by the MATLAB script, giving a change in NE and PR3 concentrations with respect to time and space (as presented in the surface plots, Figure 7). R_{max} was determined as the furthest radial distance from the centre at at which the concentration exceeded 10^{-15} M. T_{max} was determined as the latest time point at which the concentration at the centre exceeded 10^{-15} M. R_{max} and T_{max} can therefore be considered upper bounds.

Partitioning of NE and PR3 between A2M and A1AT was calculated using the final concentrations of the complexes at the end of the 0.5 s of simulated time, at which point all reactions were complete.

Results

Active site titration of enzymes

Purified PR3 and NE were active site titrated against a pure M variant A1AT of known activity (see Methods) and found to be 85% and 87% active respectively. Active enzyme concentrations were used in all subsequent calculations.

A1AT and A2M concentrations in serum samples

Serum samples were taken from subjects with various A1AT genotypes, and the concentrations of A1AT are shown in Table 1. Serum concentrations of A2M were measured and found to be similar regardless of A1AT genotype (2.8 ± 0.1 μM). Serum concentrations are within the range of previously published values (5, 6).

Inhibition assays of NSPs with serum from various A1AT genotypes using low molecular weight substrates

When serum samples were used to inhibit the activities of NE or PR3 individually, initially the enzyme activity decreased linearly as the ratio of A1AT:proteinase approached 1:1, indicating that inhibition of enzyme activity by serum largely reflected the inhibitory capacity of A1AT (Figures 1 and 2). However, when the A1AT in the serum samples was in a molar excess of the proteinase, residual proteinase activity was still observed, which was greater as the serum concentration of A1AT decreased relative to A2M. Figure 3 shows that altering the relative concentrations of pure A1AT and pure A2M produced a similar effect; reduced concentrations of A1AT relative to A2M resulted in greater residual proteinase activity even when the A1AT was in a molar excess of the proteinase. The results also demonstrate that pure A1AT alone is capable of completely inhibiting the activities of NSPs with 1:1 stoichiometry. These results demonstrate differences in partitioning of NSPs between their

371 serum inhibitors depending on their relative local concentrations, and support previously
372 published data (52) suggesting that NE bound to A2M retains its proteolytic potential, at least
373 towards low molecular weight substrates (as used in these experiments). The proteolytic
374 potential of A2M:PR3 complexes has not been studied previously, but the results presented
375 here demonstrate that A2M:PR3 complexes also retain proteolytic activity towards low
376 molecular weight substrates. The results of the experiments using purified M variant A1AT
377 and pure A2M in varying concentrations (Figure 3) did not fully replicate the results from the
378 experiments using serum (Figure 1). This suggests that the concentrations of inhibitors does
379 not solely account for the differences in partitioning of NSPs in serum samples containing
380 mutant A1AT variants (see Discussion).
381
382 The inhibition assay of NE by PiZZ serum using SlaaapN as the substrate (Figure 1) gave
383 different results to those obtained with other serum samples. Although PiZZ serum initially
384 inhibited NE activity, as the ratio of A1AT:NE increased and hence greater volumes of serum
385 (containing A2M) were present, enhanced activity of NE was detected (above that observed
386 with free NE alone). This effect was not observed when MSaapvN was used as the substrate
387 (Figure 2). Again, this effect is likely to result from NE bound to A2M, and previous authors
388 have reported enhanced activity of NE bound to A2M compared to free NE when using small
389 peptide substrates, which varies depending on the substrate used from little or no activation to
390 15-fold activation (52).
391
392 The inactivation of A2M in serum by methylamine (Figure 4) gave further confirmation that
393 the persistent proteinase activity observed when the serum A1AT was in a molar excess of
394 the proteinase was due to binding to A2M.
395

Inhibition assays of NSPs with serum or pure A1AT using elastin-fluorescein as the substrate

The activity of NE towards elastin could be fully inhibited by stoichiometric amounts of pure M variant A1AT (Figure 5A). However, when serum was used as the source of inhibitors (PiMM or PiZZ), NE activity against elastin was not completely inhibited even when A1AT was in a molar excess, suggesting that A2M:NE complexes are able to degrade elastin. However, the activity of PR3 against elastin (Figure 5B) was completely inhibited by serum (PiMM and PiZZ) in the presence of a molar excess of A1AT, suggesting that PR3 complexes with A2M are less likely to play a role in the degradation of mature elastin.

Association rate constants for A1AT variants and NSPs

The second order association rate constant (K_{ass}) values for different variants of A1AT with NE or PR3 are shown in Table 2. The values calculated for NE are comparable to previous results, with the Z variant of A1AT having a K_{ass} value which is approximately half that of the M variant (34), and the S variant of A1AT having a similar K_{ass} value compared to the M variant (35). For these experiments, it was not possible to use serum from PiFF or PiII homozygotes since no patients had been identified in the U.K. Thus, PiFZ or PiIZ heterozygotes were selected since Z A1AT made a relatively small contribution to the overall concentration of A1AT and studies have shown that A1AT from PiMZ heterozygotes has a similar K_{ass} with NE to M A1AT alone (9). Furthermore, the results presented here show that FZ A1AT has a K_{ass} value with NE comparable to that obtained with the Z variant, and are consistent with results published by Cook *et al* (9), who used partially purified F variant A1AT. More recently, we have identified a PiFF homozygote in the U.S.A, and were able to confirm our K_{ass} values reported in the current study for F variant A1AT (43). The K_{ass} values calculated in the present study demonstrate that IZ A1AT also had a reduced K_{ass} with NE

compared to M A1AT, consistent with a previous study demonstrating that purified I variant A1AT has a K_{ass} value with NE comparable to that obtained with Z A1AT (27).

For all A1AT variants studied here, the K_{ass} with NE was greater than that with PR3. The normal M variant of A1AT has a K_{ass} value for PR3 which is ten times lower than that for NE, consistent with observations published elsewhere (41). Association rate constants for PR3 and other A1AT variants have not been published previously, but the results presented here suggest that mutants of A1AT have a similar K_{ass} to the M variant. Therefore the changes in concentration of A1AT in the mutant variants are more likely to influence binding of PR3 to A1AT than changes in association rate constants.

Development of a three dimensional reaction-diffusion model

Using the calculated K_{ass} values and serum concentrations for each variant of A1AT along with published values for NE, PR3 and A2M concentrations (see Methods), we were able to construct a three dimensional reaction-diffusion model for the diffusion of NSPs from the azurophil granule following external degranulation, and their subsequent inhibition by binding to either A2M or A1AT. The aim of our model was to describe events likely to be occurring in the lung interstitium which is of particular relevance to the pathophysiology of emphysema.

The summary of the maximum diffusion distance (R_{max}) and maximum time free in solution (T_{max}) values for NSPs in the presence of different A1AT variants is shown in Figure 6, and surface plots (depicting diffusion from the azurophil granule in space and time) for NE and PR3 in the presence of either PiMM or PiZZ serum can be seen in Figure 7. The measures R_{max} and T_{max} are the distances or times at which the concentrations of the NSPs have fallen

445 below the threshold concentration of 10^{-15} M as described in Methods. They can therefore be
446 considered upper bounds.
447
448 In the presence of PiMM serum, both NE and PR3 are above the threshold concentration of
449 10^{-15} M up to a maximum distance of 8.1 μm and 22 μm respectively from the centre of the
450 azurophil granule (Figure 6A), which is also visualised in Figures 7A and 7B for NE and PR3
451 respectively. With PiZZ serum, an increase in R_{max} to 14.4 μm for NE and to 27.1 μm for
452 PR3 is predicted. An increase in R_{max} is predicted for one or both of the NSPs in all mutant
453 A1AT variants (Figure 6A), with PR3 being free at a greater distance from the centre than
454 NE (Figure 7). The maximum time free in solution (T_{max}) of PR3 and NE for each of the
455 A1AT variants is shown in Figure 6B. The PiZZ genotype exhibits the greatest T_{max} values
456 for NE (0.138 s) and PR3 (0.480 s) and the PiMM genotype exhibits the lowest T_{max} values
457 (0.041 s for NE and 0.304 s for PR3).
458
459 The R_{max} and T_{max} values for PR3 are predominantly influenced by A1AT concentration,
460 since the K_{ass} value of the A1AT:PR3 interaction is similar between A1AT variants (Table 2).
461 However, with NE, differences in K_{ass} are important in addition to A1AT concentrations. For
462 example, PiFZ serum is associated with a concentration of A1AT within the normal range of
463 PiMM serum (5), but has a reduced A1AT:NE K_{ass} value. Therefore, in the presence of PiFZ
464 serum, greater R_{max} and T_{max} values for NE are observed than with PiMM serum.
465
466 Figure 7 represents diffusion from the azurophil granule in space and time for both NE (7A
467 and 7C) and PR3 (7B and 7D) respectively, comparing the M variant (7A and 7B) to the Z
468 variant (7C and 7D) of A1AT. The results show that active PR3 diffuses to a greater distance
469 from the azurophil granule and persists for longer than NE. In the presence of the Z variant of

A1AT, there is increased activity of both NSPs (but particularly PR3) at greater distances from the azurophil granule. The presence of higher concentrations and increased time for activity in solution for both enzymes (especially PR3) will potentially allow greater proteolysis, and therefore greater local tissue damage.

Partitioning of NSPs between their inhibitors

Complex formation through binding of NE or PR3 with the inhibitors A1AT or A2M was calculated from complex concentrations when the system had reached a steady state. The percentage partitioning of PR3 and NE between A2M and variants of A1AT is shown in Figure 8. This partitioning between A2M and A1AT is important as NE and PR3 can remain active especially against small substrates when bound to A2M, and therefore may continue to contribute to tissue damage until cleared.

In the presence of PiMM serum, released NE is mostly inhibited by A1AT with a small percentage bound to A2M, similar to results reported elsewhere (37). Although the K_{ass} value for A2M:NE formation is 4.1 x 10^7 $M^{-1}s^{-1}$ (54) versus 1.45 x 10^7 $M^{-1}s^{-1}$ for A1AT:NE formation (Table 2), the concentration of A1AT is ~10 fold higher (30.3 μM against 3 μM) resulting in a greater partitioning of NE towards A1AT. With PR3, the K_{ass} value for A1AT:PR3 formation (9.24 x 10^5 $M^{-1}s^{-1}$) is ~10 fold less than the K_{ass} for A2M:PR3 formation (1.1 x 10^7 $M^{-1}s^{-1}$) (41) and this difference is greater than the difference in NE K_{ass} values. Therefore, PR3 shows an increased partitioning towards A2M, potentially leaving a greater quantity of PR3 active (at least towards low molecular weight substrates) than NE.

In the presence of PiZZ serum, a significantly increased partitioning towards A2M is predicted for both NE and PR3. For NE, this is likely to reflect the reduction in K_{ass} with the

Z variant of A1AT (Table 2) as well as the reduced A1AT concentration. The K_{ass} for PR3 and A1AT is similar between the M and Z variants and is lower than the K_{ass} with NE. Following release, NSPs (but particularly NE) rapidly deplete free Z A1AT leaving A2M to inhibit the remainder, and hence PR3 partitions more readily to A2M. A similar pattern is noticed with the other mutant A1AT variants but to a lesser extent due to their higher A1AT serum concentrations compared to the Z variant. This raises the possibility that increased partitioning towards A2M may be partially responsible for any increased tissue damage in these variant A1ATD individuals.

Discussion

The model presented here has highlighted the complex proteinase- inhibitor interactions occurring in COPD and A1ATD, where more than one enzyme is released from the azurophil granules of activated neutrophils, and the local inhibitors have different affinities for the enzymes. The results highlight a potentially important role for PR3 in the pathophysiology of emphysema due to its greater concentration in azurophil granules, its reduced K_{ass} with A1AT variants, its greater diffusion distance and time spent uninhibited in solution following release, and its greater propensity to partition to A2M where it retains proteolytic activity.

NSPs have been the best proven mediators to date replicating the pathological features of COPD and, in particular, emphysema. The interactions between NSPs and their endogenous inhibitors and substrates *in vivo* are complex and previously poorly understood. Our data provide further information on the potential radius of tissue damage by NSPs following external degranulation from azurophil granules, and their partitioning between the major serum inhibitors A1AT and A2M, both of which are found in the lung. Although the size of A2M restricts its diffusion into the airways (and possibly the lung interstitium) in the absence of inflammation (46), partitioning of NSPs to A2M is of biological importance as formation of A2M:NSP complexes does not involve direct interaction with the active site of the enzyme, and our data has shown that A2M:NE complexes retain proteolytic potential whereas A1AT:NE complexes do not (Figure 3). Indeed, active A2M:NE complexes have been implicated in the pathogenesis of emphysema in animal models (48), the adult respiratory distress syndrome (ARDS) in humans (56), and the degradation of cartilage matrix in rheumatoid arthritis (30). Our data (Figure 5) have shown that A2M:NE complexes are able to degrade elastin-fluorescein, and previous studies (29) have also shown that complexes of A2M with porcine pancreatic elastase (PPE) are capable of digesting

528 chemically solubilised elastin. However, other studies have shown that NE complexes with
529 A2M are unable to degrade mature elastin (21) although NE bound to A2M may be able to
530 degrade the elastin precursor tropoelastin (13), which is secreted into the extracellular space
531 prior to formation of the cross linkages found in elastin (42) and hence could affect the repair
532 process. Further work is therefore required to determine the presence and biological
533 significance of active A2M:NE complexes with particular reference to emphysema.
534
535 The proteolytic activity of A2M:PR3 complexes has not been reported previously, and may
536 also have clinical relevance particularly since PR3 has a lower K_{ass} than NE for all variants of
537 A1AT studied here. Therefore, in situations where the local concentration of A1AT is
538 inadequate to inhibit both proteinases, NE would be preferentially inhibited and PR3 would
539 be more likely to form a complex with A2M. Although A2M:PR3 complexes do not degrade
540 elastin (Figure 5B), active A2M:PR3 complexes may have indirect consequences for tissue
541 destruction due to their ability to activate pro-inflammatory cytokines (1). In support of this,
542 Korkmaz *et al* (20) confirmed that NE was the main target of A1AT when identical molar
543 amounts of A1AT and NSPs were present together and PR3 was only inhibited once NE had
544 been totally inhibited. The authors confirmed this for inhibitors present in broncho-alveolar
545 lavage fluid and they found that PR3 (both free and bound to the neutrophil cell membrane)
546 was the least inhibited NSP.
547
548 Our data from the model (Figure 8) indicate that PR3 would partition more to A2M than NE,
549 especially in the presence of mutant A1AT variants. However, some discrepancies are noted
550 between the data obtained from the model and the *in vitro* data using serum samples (Figure
551 2) in the presence of the F or I variants of A1AT. From the *in vitro* data, it appears that
552 partitioning of NE to A2M increased in the presence of F or I variant A1AT, which is

553 unlikely to be solely related to the local concentration of A1AT or its K_{ass} because the
554 partitioning is greater than that observed with PiZZ serum. In addition, partitioning of NE to
555 A2M appears to be greater than the partitioning of PR3 to A2M in the presence of the F or I
556 variants of A1AT. The exact reasons for these findings remain uncertain, but there are several
557 possibilities. Firstly, the A1AT:NE complexes formed by F or I variant A1AT could
558 dissociate in the presence of A2M resulting in the transfer of the enzyme from A1AT to A2M
559 as described by Ohlsson (36) using trypsin in dog serum, and Meyer *et al* (29) using PPE in
560 the presence of the two inhibitors. Secondly, the F or I variant A1AT could be at least partly
561 proteolytically inactivated by NE during the interaction, resulting in inactivated A1AT and
562 free NE (which could then bind to A2M). Further studies into the function of F and I variants
563 of A1AT and the stability of their complexes with NE are therefore necessary.
564
565 The inhibition assays using purified inhibitors in varying concentrations (Figure 3) did not
566 fully replicate the inhibition assays using serum samples (Figure 1). There are several
567 potential reasons for this discrepancy. Firstly, the experiments using purified inhibitors
568 (Figure 3) were performed to assess whether alterations in the relative concentrations of
569 A1AT and A2M affected partitioning, and for this reason, M variant A1AT was used. If
570 purified mutant variants were to be used (such as Z, S and F variants), further changes in
571 partitioning could be observed due to differences in K_{ass} with NE. Secondly, mutant variants
572 of A1AT are susceptible to conformational transitions which may further reduce the levels of
573 functional proteinase inhibitor *in vivo*. For example, the formation of loop sheet polymers
574 reduces the anti-proteinase capabilities of mutant variants of A1AT beyond that expected for
575 the reduced concentration and K_{ass} (11). Other conformational transitions of mutant variants
576 of A1AT which may affect their anti-proteinase function *in vivo* include the formation of
577 unstable intermediates, latent A1AT or cleaved A1AT following its interaction with NSPs

578 (25). The presence of these conformations of A1AT in the serum samples would influence
579 the partitioning of NSPs more towards binding to A2M.
580
581 The inhibition assay of NE by PiZZ serum using SlaaapN as the substrate (Figure 1) showed
582 enhanced activity of NE (above that observed with free NE alone) as greater volumes of
583 serum (and hence A2M) were added. This phenomenon has been reported previously by
584 Twumasi *et al* (52). They reported that the K_m, which reflects the affinity of the enzyme for
585 the substrate, was not affected by A2M despite the marked enhancement in the catalytic
586 efficiency of the enzyme as measured by K_{cat}. They hypothesized that the conformational
587 change in A2M during entrapment of the enzyme uncovers a hydrophobic cavity which, in
588 conjunction with a positively charged group, orientates the substrate into a position which is
589 more favourable for the enzyme. However, this enhancement of NE activity was not seen
590 when MSaapvN was used as the substrate. The authors demonstrated that the degree of
591 activation of NE bound to A2M varied depending on the synthetic peptide substrate used, and
592 varied from little or no activation to 15-fold activation. Interestingly, they also showed that
593 the activity of PPE towards SlaaapN was inhibited by human A2M, thus highlighting species
594 differences in enzyme inhibition and kinetics towards synthetic peptide substrates.
595
596 When comparing the results of the inhibition assays using low molecular weight substrates
597 (Figures 1 and 2) with those using elastin as the substrate (Figure 5), it appears that A2M:NE
598 complexes may be less active towards elastin than against low molecular weight peptide
599 substrates. The residual activities of NE (which represent the activities of A2M:NE
600 complexes since the A1AT was in a molar excess) were greater when peptide substrates were
601 used compared to elastin. These findings are consistent with those reported elsewhere (30)
602 and could possibly be due to a proportion of the complexes containing two molecules of NE,

603 which would not allow simultaneous activity of these two NE molecules towards a
604 macromolecular substrate such as elastin.
605
606 The results from the three dimensional reaction-diffusion model (Figure 7) show that NSPs
607 are able to travel up to 27 μm from the site of release. In the presence of the normal PiMM
608 genotype, the NSPs are confined to a relatively small area of activity. However, in the
609 presence of mutant A1AT variants, the R_{max} increases and hence the radius at which NSPs are
610 enzymatically active. This is consistent with the increased tissue destruction and early onset
611 emphysema observed in PiZZ homozygotes. The use of a radially-symmetric model for NE
612 diffusion has previously been tested experimentally (23) and shows high concordance with
613 the current model. The authors demonstrated how degranulation of azurophil granules could
614 significantly damage a substrate surface as a neutrophil passes across it even in the presence
615 of inhibitors. This suggests that if a neutrophil is close to or adherent to a surface, NSP
616 release from an azurophil granule can cause significant tissue degradation, which would be
617 amplified in the presence of mutant variants of A1AT. In addition, in the presence of
618 infection or increased inflammation in the lung, an influx of neutrophils would result in a
619 large amount of proteinase release, thereby depleting local inhibitors still further.
620
621 Our data (Figure 6) suggest that R_{max} and T_{max} values for both NE and PR3 are influenced by
622 the local A1AT concentration, although K_{ass} values are also important especially when
623 considering NE activity. This relationship between the radius of potential tissue destruction
624 surrounding the azurophil granules and local A1AT concentration may have significance for
625 one of the treatment methods for A1ATD. In A1ATD individuals, particularly those with the
626 PiZZ phenotype, augmentation therapy with pooled human A1AT reduces the decline in lung
627 density as measured by CT scanning (47). A serum A1AT concentration of 11 μM has been

628 deemed to be the “protective threshold”, below which A1AT augmentation should be
629 considered (51). In the current study, small but significantly increased R_{max} values have also
630 been determined for the PiIZ, PiFZ, PiMZ and PiSS genotypes, which have serum A1AT
631 concentrations above the 11 μM threshold. Whether these increased R_{max} values would be
632 clinically significant enough to warrant augmentation therapy is not clear at present.
633 However, importantly, it emphasises that the potential radius of activity for PR3 exceeds that
634 for NE, and although A1AT augmentation therapy would beneficially limit activities of both
635 enzymes adding maximum protection, the same would not be true for specific NE inhibitors.
636
637 Despite the novel data generated by the model presented here, there are some limitations
638 which may have implications for any conclusions drawn for events taking place *in vivo*.
639 Firstly, this model has not considered the contribution of the chelonianin inhibitors produced
640 locally in the lungs, SLPI (a reversible inhibitor of NE but not PR3) and elafin (a reversible
641 inhibitor of NE and PR3). Since SLPI does not inhibit PR3 (4), incorporation of this inhibitor
642 into the model may result in an even greater role for PR3 in the pathogenesis of COPD
643 especially in A1ATD. However, SLPI is predominantly present in the upper airways (55) and
644 may play a less important role in the anti-proteinase protection of the distal airways where
645 emphysema occurs, although SLPI has been identified in the lung interstitium associated with
646 elastin (58). Secondly, the model does not incorporate any elimination kinetics of A2M:NSP
647 complexes from the system. Since NSPs remain active when bound to A2M, this may affect
648 extracellular matrix degradation in the lung interstitium due to circulation of lymph. Thirdly,
649 the model does not consider any potential binding of NSPs to the neutrophil cell membrane.
650 Membrane-bound NSPs remain catalytically active towards both synthetic peptide and high
651 molecular weight biological substrates (8, 39), although this activity can be inhibited by
652 stoichiometric amounts of A1AT (17, 19). The quantity and affinity of cell membrane

653 binding of NSPs remains unknown. However, the model assumes equal affinities of the
654 degranulated NSPs for the cell membrane which would retain the differential concentrations
655 of the remaining NE and PR3. Finally, the model does not incorporate the third most
656 common NSP, cathepsin G. Although this NSP does not produce emphysema-like lesions in
657 animal and *in vitro* studies, it would provide a further competing target for A1AT.
658 Importantly, however, the K_{ass} value for cathepsin G and M variant A1AT is more than one
659 hundred fold lower than that of NE, and about tenfold lower than that of PR3 (3, 41) and
660 therefore A1AT would be expected to bind cathepsin G only after the other NSPs have been
661 inhibited. Likewise, the K_{ass} value of the cathepsin G-A2M interaction is approximately
662 tenfold lower than that of the other NSPs (54) and therefore its inclusion in the model would
663 be unlikely to affect the predictions reported for the other NSPs. These caveats highlight
664 further areas of research required in order to gain a greater understanding of the complex
665 proteinase/anti-proteinase imbalance occurring *in vivo* especially in subjects with emphysema
666 with or without A1AT variants. An increased understanding of the pathogenesis may aid the
667 future development of novel therapies for COPD in general and A1ATD in particular.
668
669 In conclusion, the results presented here have provided a greater insight into the proteinase-
670 inhibitor interactions occurring in COPD and A1ATD. The data suggest that PR3 may be
671 more important in the pathophysiology of COPD than previously considered due to the
672 greater quantities stored in azurophil granules, its reduced K_{ass} with A1AT variants and
673 greater potential radius of activity. In addition, when NSPs form complexes with A2M, they
674 retain their activities, which may have direct (tissue destruction) or indirect (activation of pro-
675 inflammatory cytokines) effects *in vivo*. Finally, local A1AT concentrations regulate NSP
676 activities, which may have implications for A1AT augmentation therapy in A1ATD
677 individuals.

Acknowledgements

The computations described in this paper were performed using the University of Birmingham's BlueBEAR HPC service, which was purchased through HEFCE SRIF-3 funds. See http://www.bear.bham.ac.uk for more details.

Conflict of interest

NJS has received funding for travel to conferences from GlaxoSmithKline, Boehringer Ingelheim and Napp Pharmaceuticals. MJB none declared. DS none declared. JUK none declared. TD none declared. RAS has sat on advisory boards for CSL, Kamada and Grifols; has received lecture fees from CSL and Grifols, and has received unrestricted research grants from CSL and Grifols.

References

1. **Bank U, and Ansorge S**. More than destructive: neutrophil-derived serine proteases in cytokine bioactivity control. *Journal of leukocyte biology* 69: 197-206, 2001.
2. **Baur X, and Bencze K**. Study of familial alpha-1-proteinase inhibitor deficiency including a rare proteinase inhibitor phenotype (IZ). I. Alpha-1-phenotyping and clinical investigations. *Respiration; international review of thoracic diseases* 51: 188-195, 1987.
3. **Beatty K, Bieth J, and Travis J**. Kinetics of association of serine proteinases with native and oxidized alpha-1-proteinase inhibitor and alpha-1-antichymotrypsin. *The Journal of biological chemistry* 255: 3931-3934, 1980.
4. **Bergenfeldt M, Axelsson L, and Ohlsson K**. Release of neutrophil proteinase 4(3) and leukocyte elastase during phagocytosis and their interaction with proteinase inhibitors. *Scandinavian journal of clinical and laboratory investigation* 52: 823-829, 1992.
5. **Brantly ML, Wittes JT, Vogelmeier CF, Hubbard RC, Fells GA, and Crystal RG**. Use of a highly purified alpha 1-antitrypsin standard to establish ranges for the common normal and deficient alpha 1-antitrypsin phenotypes. *Chest* 100: 703-708, 1991.
6. **Bristow CL, Di Meo F, and Arnold RR**. Specific activity of alpha1proteinase inhibitor and alpha2macroglobulin in human serum: application to insulin-dependent diabetes mellitus. *Clinical immunology and immunopathology* 89: 247-259, 1998.
7. **Campbell EJ, Campbell MA, Boukedes SS, and Owen CA**. Quantum proteolysis by neutrophils: implications for pulmonary emphysema in alpha 1-antitrypsin deficiency. *The Journal of clinical investigation* 104: 337-344, 1999.
8. **Campbell EJ, Campbell MA, and Owen CA**. Bioactive proteinase 3 on the cell surface of human neutrophils: quantification, catalytic activity, and susceptibility to inhibition. *J Immunol* 165: 3366-3374, 2000.
9. **Cook L, Burdon JG, Brenton S, Knight KR, and Janus ED**. Kinetic characterisation of alpha-1-antitrypsin F as an inhibitor of human neutrophil elastase. *Pathology* 28: 242-247, 1996.
10. **Doll R, Peto R, Wheatley K, Gray R, and Sutherland I**. Mortality in relation to smoking: 40 years' observations on male British doctors. *BMJ (Clinical research ed* 309: 901-911, 1994.
11. **Elliott PR, Bilton D, and Lomas DA**. Lung polymers in Z alpha1-antitrypsin deficiency-related emphysema. *American journal of respiratory cell and molecular biology* 18: 670-674, 1998.
12. **Eriksson S**. Pulmonary Emphysema and Alpha1-Antitrypsin Deficiency. *Acta medica Scandinavica* 175: 197-205, 1964.
13. **Galdston M, Levytska V, Liener IE, and Twumasi DY**. Degradation of tropoelastin and elastin substrates by human neutrophil elastase, free and bound to alpha2-macroglobulin in serum of the M and Z (Pi) phenotypes for alpha1-antitrypsin. *The American review of respiratory disease* 119: 435-441, 1979.
14. **Kao RC, Wehner NG, Skubitz KM, Gray BH, and Hoidal JR**. Proteinase 3. A distinct human polymorphonuclear leukocyte proteinase that produces emphysema in hamsters. *The Journal of clinical investigation* 82: 1963-1973, 1988.
15. **Kelly CP, Tyrrell DN, McDonald GS, Whitehouse DB, and Prichard JS**. Heterozygous FZ alpha 1 antitrypsin deficiency associated with severe emphysema and hepatic disease: case report and family study. *Thorax* 44: 758-759, 1989.
16. **Koj A, Regoeczi E, Toews CJ, Leveille R, and Gauldie J**. Synthesis of antithrombin III and alpha-1-antitrypsin by the perfused rat liver. *Biochimica et biophysica acta* 539: 496-504, 1978.

17. **Korkmaz B, Attucci S, Jourdan ML, Juliano L, and Gauthier F**. Inhibition of neutrophil elastase by alpha1-protease inhibitor at the surface of human polymorphonuclear neutrophils. *J Immunol* 175: 3329-3338, 2005.
18. **Korkmaz B, Attucci S, Juliano MA, Kalupov T, Jourdan ML, Juliano L, and Gauthier F**. Measuring elastase, proteinase 3 and cathepsin G activities at the surface of human neutrophils with fluorescence resonance energy transfer substrates. *Nat Protoc* 3: 991-1000, 2008.
19. **Korkmaz B, Jaillet J, Jourdan ML, Gauthier A, Gauthier F, and Attucci S**. Catalytic activity and inhibition of wegener antigen proteinase 3 on the cell surface of human polymorphonuclear neutrophils. *The Journal of biological chemistry* 284: 19896-19902, 2009.
20. **Korkmaz B, Poutrain P, Hazouard E, de Monte M, Attucci S, and Gauthier FL**. Competition between elastase and related proteases from human neutrophil for binding to alpha1-protease inhibitor. *American journal of respiratory cell and molecular biology* 32: 553-559, 2005.
21. **Kueppers F, Abrams WR, Weinbaum G, and Rosenbloom J**. Resistance of tropoelastin and elastin peptides to degradation by alpha 2-macroglobulin-protease complexes. *Archives of biochemistry and biophysics* 211: 143-150, 1981.
22. **Liou TG, and Campbell EJ**. Nonisotropic enzyme--inhibitor interactions: a novel nonoxidative mechanism for quantum proteolysis by human neutrophils. *Biochemistry* 34: 16171-16177, 1995.
23. **Liou TG, and Campbell EJ**. Quantum proteolysis resulting from release of single granules by human neutrophils: a novel, nonoxidative mechanism of extracellular proteolytic activity. *J Immunol* 157: 2624-2631, 1996.
24. **Lomas DA, Evans DL, Finch JT, and Carrell RW**. The mechanism of Z alpha 1-antitrypsin accumulation in the liver. *Nature* 357: 605-607, 1992.
25. **Lomas DA, and Mahadeva R**. Alpha1-antitrypsin polymerization and the serpinopathies: pathobiology and prospects for therapy. *The Journal of clinical investigation* 110: 1585-1590, 2002.
26. **Lucey EC, Stone PJ, Breuer R, Christensen TG, Calore JD, Catanese A, Franzblau C, and Snider GL**. Effect of combined human neutrophil cathepsin G and elastase on induction of secretory cell metaplasia and emphysema in hamsters, with in vitro observations on elastolysis by these enzymes. *The American review of respiratory disease* 132: 362-366, 1985.
27. **Mahadeva R, Chang WS, Dafforn TR, Oakley DJ, Foreman RC, Calvin J, Wight DG, and Lomas DA**. Heteropolymerization of S, I, and Z alpha1-antitrypsin and liver cirrhosis. *The Journal of clinical investigation* 103: 999-1006, 1999.
28. **Mast AE, Enghild JJ, Pizzo SV, and Salvesen G**. Analysis of the plasma elimination kinetics and conformational stabilities of native, proteinase-complexed, and reactive site cleaved serpins: comparison of alpha 1-proteinase inhibitor, alpha 1-antichymotrypsin, antithrombin III, alpha 2-antiplasmin, angiotensinogen, and ovalbumin. *Biochemistry* 30: 1723-1730, 1991.
29. **Meyer JF, Bieth J, and Metais P**. On the inhibition of elastase by serum. Some distinguishing properties of alpha1-antitrypsin and alpha2-macroglobulin. *Clin Chim Acta* 62: 43-53, 1975.
30. **Moore AR, Appelboam A, Kawabata K, Da Silva JA, D'Cruz D, Gowland G, and Willoughby DA**. Destruction of articular cartilage by alpha 2 macroglobulin elastase complexes: role in rheumatoid arthritis. *Ann Rheum Dis* 58: 109-113, 1999.
31. **Morton KW, and Mayers DF**. *Numerical solution of partial differential equations (second edition)*. Cambridge: 2005.

32. **MRC**. Definition and classification of chronic bronchitis for clinical and epidemiological purposes. A report to the Medical Research Council by their Committee on the Aetiology of Chronic Bronchitis. *Lancet* 1: 775-779, 1965.
33. **Musumeci V, Vincenti A, and Bizzi B**. A method for the differential determination of plasma antithrombins. *J Clin Pathol* 29: 63-68, 1976.
34. **Ogushi F, Fells GA, Hubbard RC, Straus SD, and Crystal RG**. Z-type alpha 1-antitrypsin is less competent than M1-type alpha 1-antitrypsin as an inhibitor of neutrophil elastase. *The Journal of clinical investigation* 80: 1366-1374, 1987.
35. **Ogushi F, Hubbard RC, Fells GA, Casolaro MA, Curiel DT, Brantly ML, and Crystal RG**. Evaluation of the S-type of alpha-1-antitrypsin as an in vivo and in vitro inhibitor of neutrophil elastase. *The American review of respiratory disease* 137: 364-370, 1988.
36. **Ohlsson K**. Comparison of affinity of trypsin for two -macroglobulin fractions and for 1 -antitrypsin in dog serum. *Clin Chim Acta* 32: 215-220, 1971.
37. **Ohlsson K, and Olsson I**. Neutral proteases of human granulocytes. III. Interaction between human granulocyte elastase and plasma protease inhibitors. *Scandinavian journal of clinical and laboratory investigation* 34: 349-355, 1974.
38. **Oldham PD**. Measurement of the prevalence of emphysema. Problems of definition and sampling. *Proc R Soc Med* 69: 127-128, 1976.
39. **Owen CA, Campbell MA, Sannes PL, Boukedes SS, and Campbell EJ**. Cell surface-bound elastase and cathepsin G on human neutrophils: a novel, non-oxidative mechanism by which neutrophils focus and preserve catalytic activity of serine proteinases. *J Cell Biol* 131: 775-789, 1995.
40. **Pauwels RA, and Rabe KF**. Burden and clinical features of chronic obstructive pulmonary disease (COPD). *Lancet* 364: 613-620, 2004.
41. **Rao NV, Wehner NG, Marshall BC, Gray WR, Gray BH, and Hoidal JR**. Characterization of proteinase-3 (PR-3), a neutrophil serine proteinase. Structural and functional properties. *The Journal of biological chemistry* 266: 9540-9548, 1991.
42. **Ross R, and Bornstein P**. Elastic fibers in the body. *Scientific American* 224: 44-52, 1971.
43. **Sinden NJ, Koura F, and Stockley RA**. The significance of the F variant of alpha-1-antitrypsin and unique case report of a PiFF homozygote. *BMC pulmonary medicine* 14: 132, 2014.
44. **Sinden NJ, and Stockley RA**. Proteinase 3 activity in sputum from subjects with Alpha-1-Antitrypsin deficiency and COPD. *Eur Respir J* 41: 1042-1050, 2013.
45. **Stockley RA**. Neutrophils and the pathogenesis of COPD. *Chest* 121: 151S-155S, 2002.
46. **Stockley RA, Mistry M, Bradwell AR, and Burnett D**. A study of plasma proteins in the sol phase of sputum from patients with chronic bronchitis. *Thorax* 34: 777-782, 1979.
47. **Stockley RA, Parr DG, Piitulainen E, Stolk J, Stoel BC, and Dirksen A**. Therapeutic efficacy of alpha-1 antitrypsin augmentation therapy on the loss of lung tissue: an integrated analysis of 2 randomised clinical trials using computed tomography densitometry. *Respiratory research* 11: 136, 2010.
48. **Stone PJ, Calore JD, Snider GL, and Franzblau C**. Role of alpha-macroglobulin-elastase complexes in the pathogenesis of elastase-induced emphysema in hamsters. *The Journal of clinical investigation* 69: 920-931, 1982.
49. **Tashkin DP, Clark VA, Coulson AH, Simmons M, Bourque LB, Reems C, Detels R, Sayre JW, and Rokaw SN**. The UCLA population studies of chronic obstructive respiratory disease. VIII. Effects of smoking cessation on lung function: a prospective study of a free-living population. *The American review of respiratory disease* 130: 707-715, 1984.

50. **Travis J**. Structure, function, and control of neutrophil proteinases. *The American journal of medicine* 84: 37-42, 1988.
51. **Turino GM, Barker AF, Brantly ML, Cohen AB, Connelly RP, Crystal RG, Eden E, Schluchter MD, and Stoller JK**. Clinical features of individuals with PI*SZ phenotype of alpha 1-antitrypsin deficiency. alpha 1-Antitrypsin Deficiency Registry Study Group. *American journal of respiratory and critical care medicine* 154: 1718-1725, 1996.
52. **Twumasi DY, Liener IE, Galdston M, and Levytska V**. Activation of human leukocyte elastase by human alpha2-macroglobulin. *Nature* 267: 61-63, 1977.
53. **Tyn MT, and Gusek TW**. Prediction of diffusion coefficients of proteins. *Biotechnol Bioeng* 35: 327-338, 1990.
54. **Virca GD, and Travis J**. Kinetics of association of human proteinases with human alpha 2-macroglobulin. *The Journal of biological chemistry* 259: 8870-8874, 1984.
55. **Vogelmeier C, Hubbard RC, Fells GA, Schnebli HP, Thompson RC, Fritz H, and Crystal RG**. Anti-neutrophil elastase defense of the normal human respiratory epithelial surface provided by the secretory leukoprotease inhibitor. *The Journal of clinical investigation* 87: 482-488, 1991.
56. **Wewers MD, Herzyk DJ, and Gadek JE**. Alveolar fluid neutrophil elastase activity in the adult respiratory distress syndrome is complexed to alpha-2-macroglobulin. *The Journal of clinical investigation* 82: 1260-1267, 1988.
57. **Wiesner O, Litwiller RD, Hummel AM, Viss MA, McDonald CJ, Jenne DE, Fass DN, and Specks U**. Differences between human proteinase 3 and neutrophil elastase and their murine homologues are relevant for murine model experiments. *FEBS letters* 579: 5305-5312, 2005.
58. **Willems LN, Otto-Verberne CJ, Kramps JA, ten Have-Opbroek AA, and Dijkman JH**. Detection of antileukoprotease in connective tissue of the lung. *Histochemistry* 86: 165-168, 1986.
59. **Ying QL, and Simon SR**. Elastolysis by proteinase 3 and its inhibition by alpha(1)-proteinase inhibitor: a mechanism for the incomplete inhibition of ongoing elastolysis. *American journal of respiratory cell and molecular biology* 26: 356-361, 2002.
60. **Zaher C, Halbert R, Dubois R, George D, and Nonikov D**. Smoking-related diseases: the importance of COPD. *Int J Tuberc Lung Dis* 8: 1423-1428, 2004.

Figure legends

Figure 1- Inhibition of NE activity by serum from various A1AT genotypes

Inhibition of NE activity by PiMM, PiFZ and PiZZ sera using SlaaapN as the substrate. The x-axis shows the molar ratio of serum A1AT to active NE. Initially, NE activity decreases linearly as the ratio of A1AT:proteinase approaches 1:1, indicating that NE inhibition largely reflects the inhibitory capacity of A1AT in serum. The residual NE activity observed when serum A1AT is in a molar excess reflects partitioning of the enzyme to A2M where it retains proteolytic activity (and shows enhanced activity in the presence of PiZZ serum). This phenomenon is greater as the serum A1AT concentration reduces relative to A2M. The SEM is small and falls within the symbol.

Figure 2- Inhibition of NE or PR3 activities by serum from various A1AT genotypes

Inhibition of NE (A) or PR3 (B) activity by PiMM, PiFZ, PiIZ and PiZZ sera using MSaapvN rather than SlaaapN as the substrate. Initially, NSP activity decreases linearly as the ratio of A1AT:proteinase approaches 1:1, indicating that NSP inhibition largely reflects the inhibitory capacity of A1AT in serum. The residual NSP activity observed when serum A1AT is in a molar excess reflects partitioning of the enzyme to A2M, and this phenomenon is greater in the presence of mutant variants of A1AT. The SEM is small and falls within the symbol.

Figure 3- Inhibition of NE with mixtures of pure A2M and pure M variant A1AT in concentrations equivalent to those found in serum from various A1AT genotypes

Inhibition assays of NE using purified inhibitors in concentrations equivalent to those found in PiMM, PiFZ and PiZZ sera, and SlaaapN as the substrate. The results show that altering the relative concentrations of pure A1AT and pure A2M produces a similar effect to that

observed with serum samples, with the greatest residual NE activity being observed when inhibitors are used in proportions equivalent to PiZZ serum. The reduced concentration of A1AT relative to A2M (as found with mutant A1AT variants) results in greater residual NE activity when the A1AT is in a molar excess of NE, suggesting greater partitioning of NE to A2M where the enzyme remains active. Pure A1AT alone (square points) is capable of completely inhibiting NE activity. The SEM is small and falls within the symbol.

Figure 4- Inhibition of NE activity by serum samples with or without treatment with methylamine

Inhibition of NE using PiMM (A) or PiZZ (B) serum samples with or without treatment with methylamine, using SlaaapN as the substrate. Following inactivation of A2M in the serum samples by methylamine, NE activity is fully inhibited by serum A1AT.

Figure 5- Inhibition of NE or PR3 activities by serum samples or pure A1AT using elastin-fluorescein as the substrate

Inhibition of NE (A) or PR3 (B) activity by PiMM or PiZZ sera or pure A1AT using elastin-fluorescein as the substrate. The results show that pure A1AT was able to completely inhibit NE activity against elastin-fluorescein. However, when serum was used as the source of inhibitors, NE activity against elastin was not completely inhibited even when A1AT was in a molar excess, suggesting that A2M:NE complexes are also able to degrade elastin. The activity of PR3 against elastin could be completely inhibited by PiMM and PiZZ sera. Graph A shows the mean results of 3 experiments and error bars indicate the SEM. Graph B shows the results from single experiments.

Figure 6- Maximum distance (R_{max}) and maximum time (T_{max}) at which free NE or PR3 are present in the reaction-diffusion model

Maximum distance (R_{max}) (A) and maximum time (T_{max}) (B) at which free NE or PR3 are above a threshold of 10^{-15} M in the reaction-diffusion model using the K_{ass} values and serum concentrations of A1AT for each variant. PR3 activity would be present at greater distances, and PR3 would become inhibited later than NE. Mutant A1AT variants result in greater R_{max} and T_{max} values compared to the M variant.

Figure 7- Surface plots for NE and PR3 in the presence of PiMM or PiZZ serum

A surface representation of the $\log_{10}$ of the concentration of active NE or PR3 at a given radius from the centre of the azurophil granule (μm) and in time (s). M and Z variants of A1AT are detailed, as these show the extremes of the variants simulated in this model. White regions correspond to concentrations below the threshold value of 10^{-15} M. Plots show detailed results as follows: (A) NE in PiMM serum, (B) PR3 in PiMM serum, (C) NE in PiZZ serum, and (D) PR3 in PiZZ serum. The plots show that active PR3 diffuses to a greater distance from the azurophil granule than NE, and that both NE and PR3 activity would be above a threshold of 10^{-15} M at greater distances in the presence of PiZZ serum compared to PiMM serum. This pattern is also observed in time, where active PR3 would be present for longer than NE, especially in the presence of PiZZ serum.

Figure 8- Partitioning of NSPs between inhibitors in the presence of different A1AT variants

Percentage partitioning of NE (A) and PR3 (B) between A2M and variants of A1AT. The PiZZ genotype exhibits the greatest change in partitioning of all the mutant variants, with increased partitioning of NSPs towards A2M.

944 Table 1- A1AT serum concentrations

A1AT genotype	Serum A1AT concentration (μM)
PiMM	30.3
PiSS	14.4
PiFZ	21.6
PiIZ	16.6
PiZZ	4.3

945 A1AT: alpha-1-antitrypsin

946

947 Table 2- Association rate constants for A1AT variants with NE or PR3

A1AT variant	**Association rate constant with NE (Mean ± SEM) at 23°C (M^{-1} s^{-1})**	**Association rate constant with PR3 (Mean ± SEM) at 23°C (M^{-1} s^{-1})**
M	(1.45 ± 0.02) x 10^7	(9.24 ± 0.48) x 10^5
S	(1.14 ± 0.36) x 10^7	(9.51 ± 3.00) x 10^5
Z	(7.34 ± 0.03) x 10^6	(1.10 ± 0.21) x 10^6
FZ	(5.75 ± 1.43) x 10^6	(1.43 ± 0.29) x 10^6
IZ	(8.64 ± 1.22) x 10^6	(1.00 ± 0.12) x 10^6

948 A1AT: alpha-1-antitrypsin, NE: neutrophil elastase, PR3: proteinase 3, SEM: standard error

949 of the mean

950

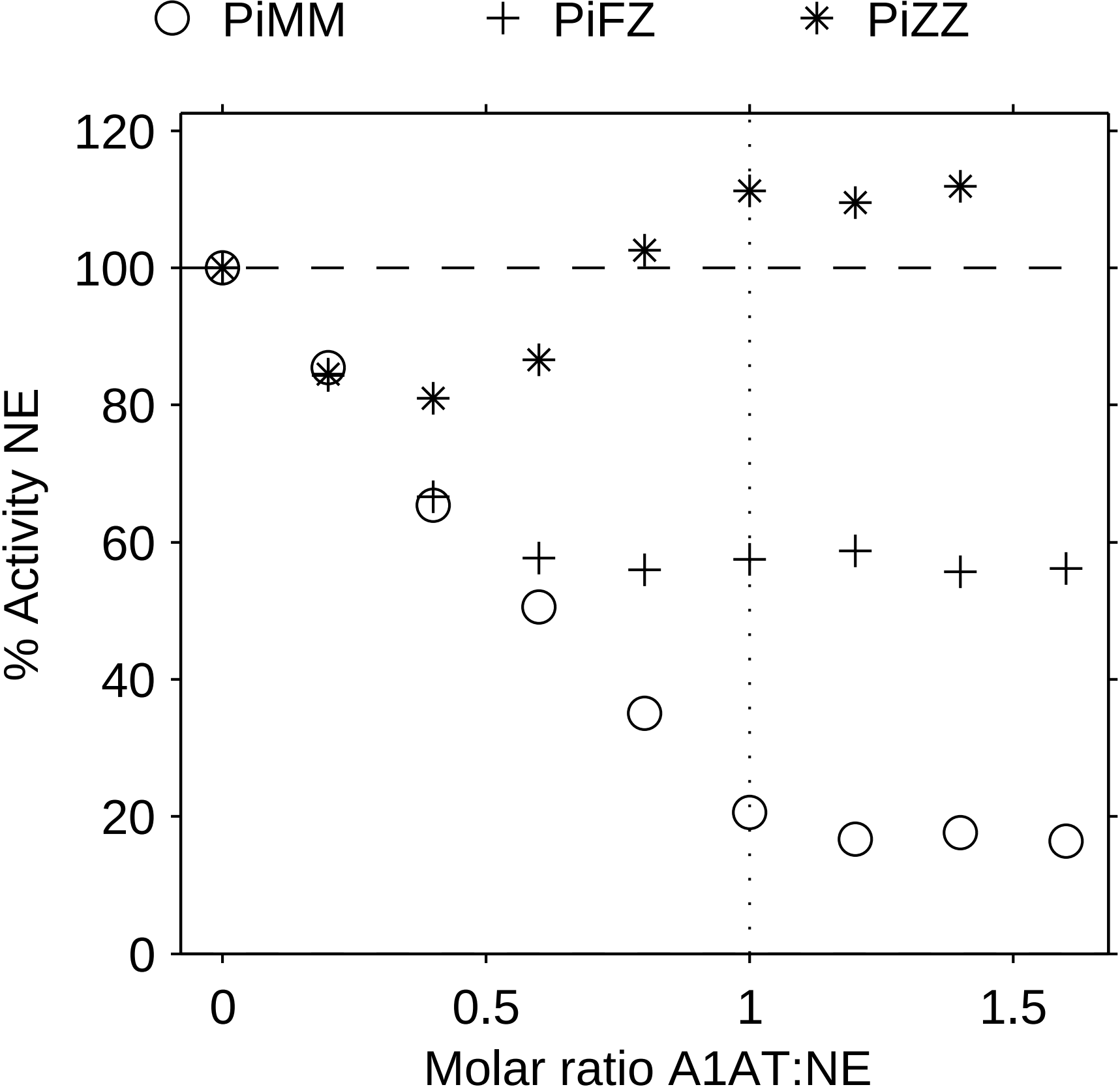
PiMM
PiFZ
PiZZ
120
100
80
60
40
20
0
% Activity NE
0
0.5
1
1.5
Molar ratio A1AT:NE

A

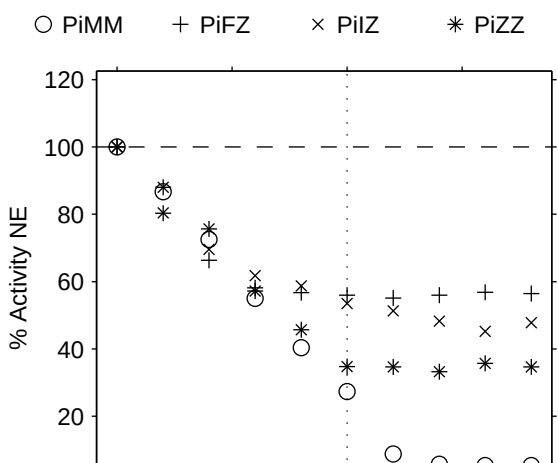
PiMM
PiFZ
PiIZ
PiZZ
% Activity NE
120
100
80
60
40
20
0
0
0.5
1
1.5
Molar ratio A1AT:NE

B

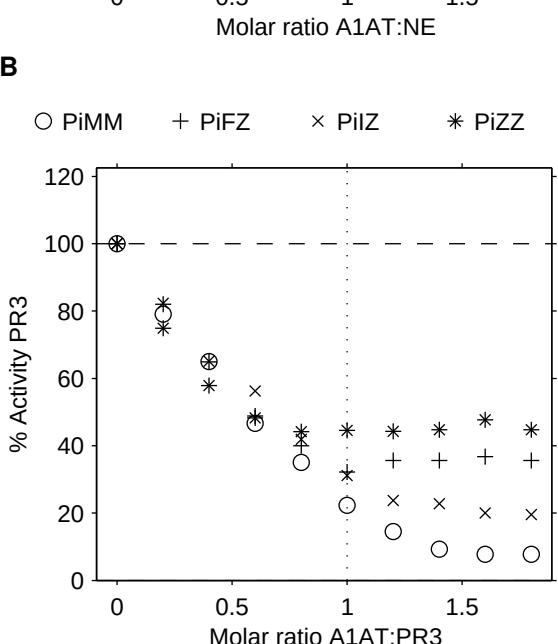
PiMM
PiFZ
PiIZ
PiZZ
% Activity PR3
120
100
80
60
40
20
0
0
0.5
1
1.5
Molar ratio A1AT:PR3

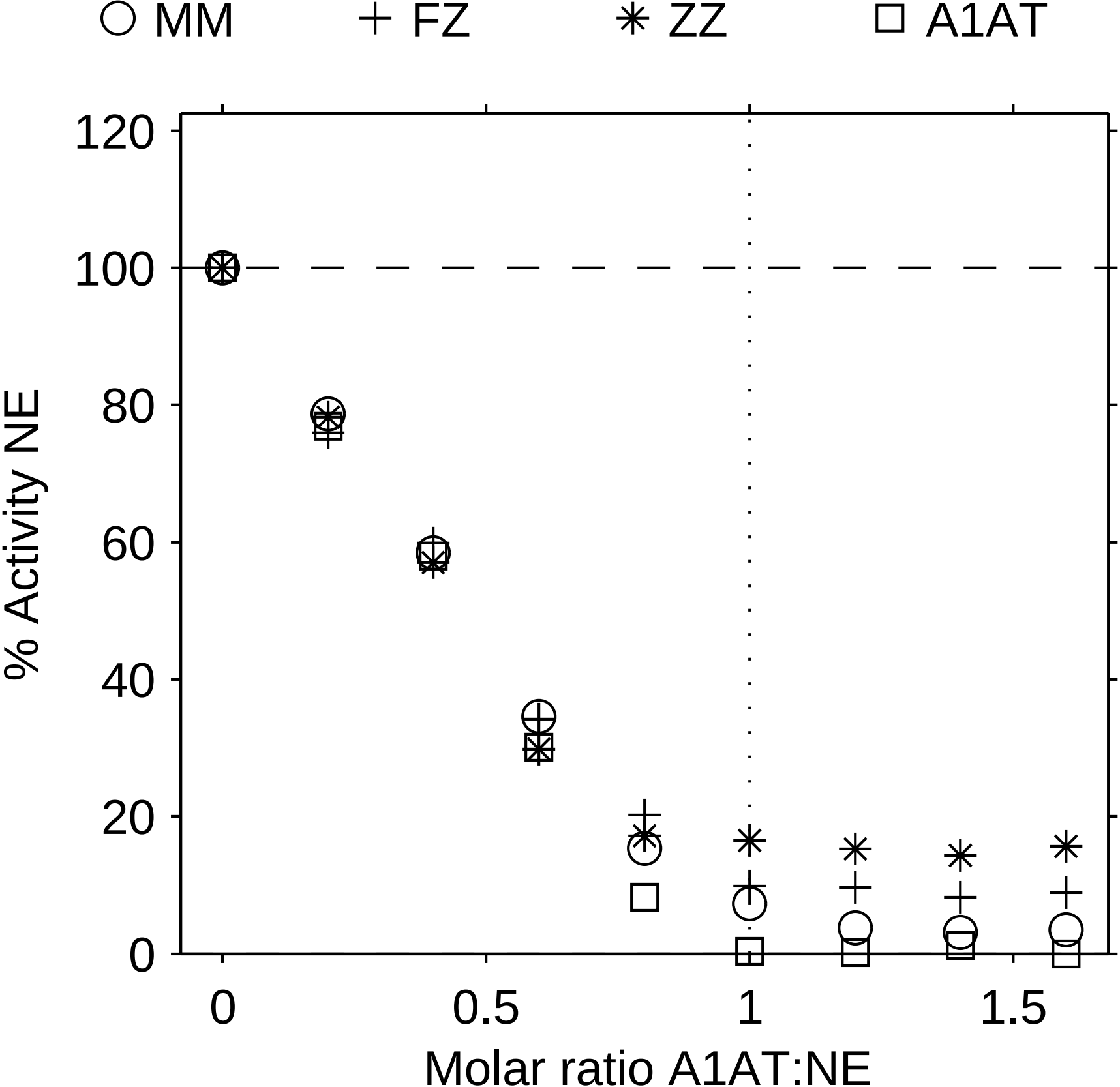
MM
FZ
ZZ
A1AT
120
100
80
60
40
20
0
% Activity NE
0
0.5
1
1.5
Molar ratio A1AT:NE

A

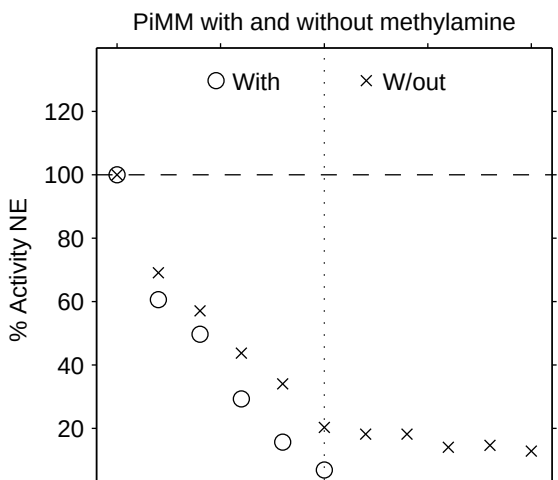
PiMM with and without methylamine
With
W/out
% Activity NE
120
100
80
60
40
20
0
0
0.5
1
1.5
2
Molar ratio A1AT:NE

B

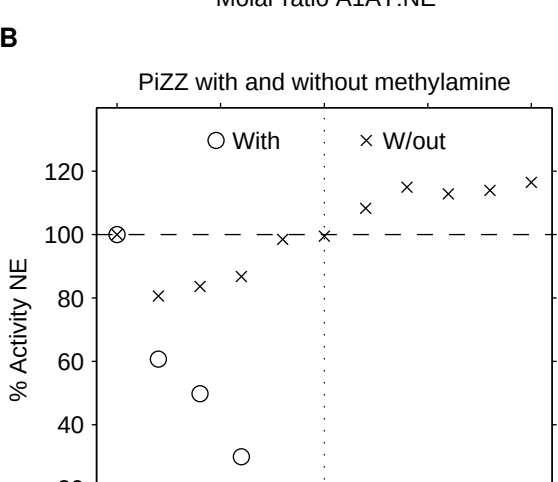
PiZZ with and without methylamine
With
W/out
% Activity NE
120
100
80
60
40
20
0
0
0.5
1
1.5
2
Molar ratio A1AT:NE

A

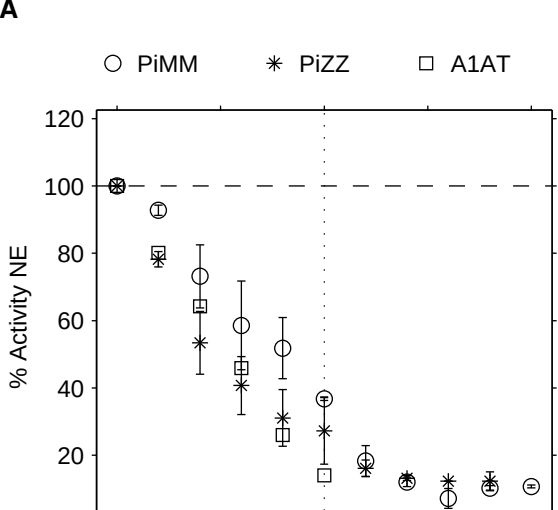
PiMM
PiZZ
A1AT
% Activity NE
120
100
80
60
40
20
0
0
0.5
1
1.5
2
Molar ratio A1AT:NE

B

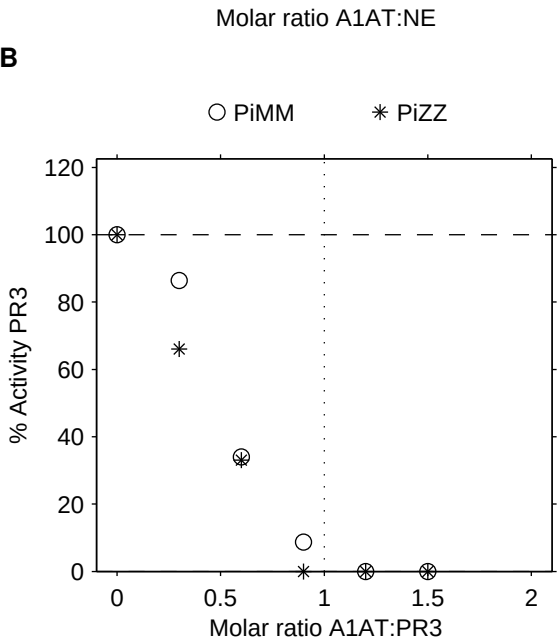
PiMM
PiZZ
% Activity PR3
120
100
80
60
40
20
0
0
0.5
1
1.5
2
Molar ratio A1AT:PR3

A

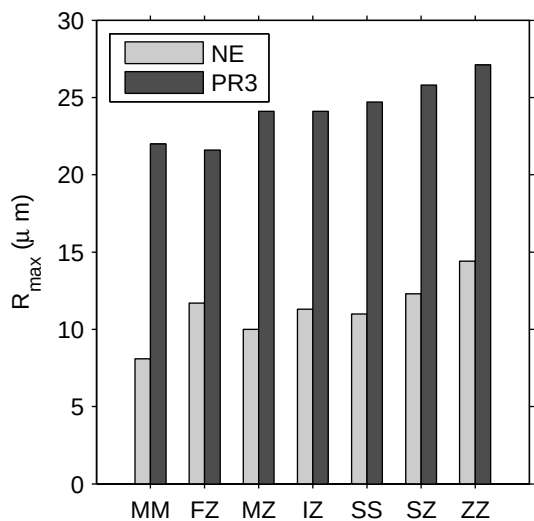
30
25
20
15
10
5
0
NE
PR3
R_{max} (μ m)
MM
FZ
MZ
IZ
SS
SZ
ZZ
A1AT genotype

B

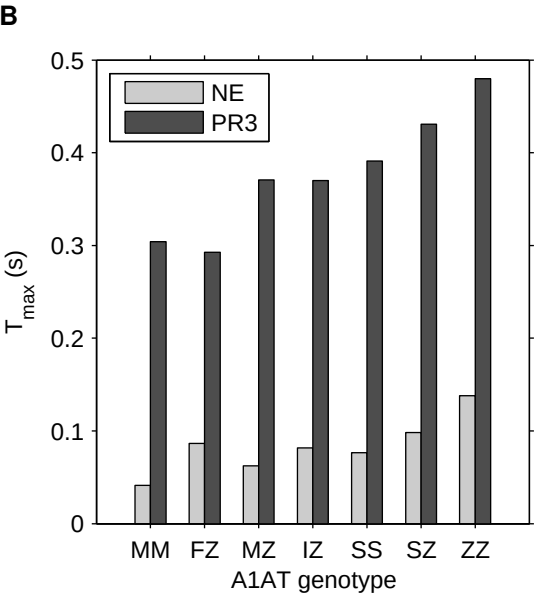
0.5
0.4
0.3
0.2
0.1
0
NE
PR3
T_{max} (s)
MM
FZ
MZ
IZ
SS
SZ
ZZ
A1AT genotype

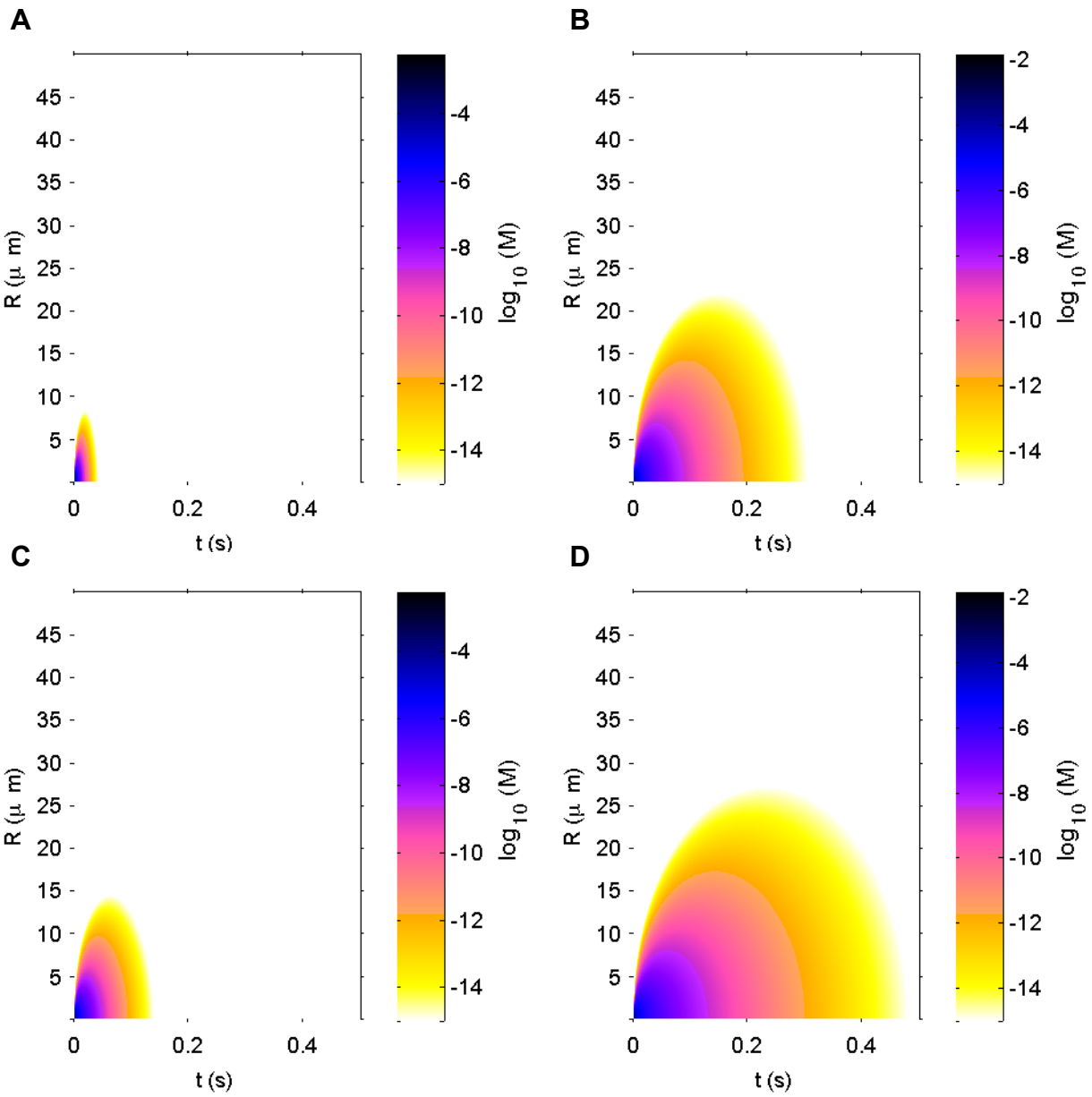
A
B
C
D
R (μ m)
t (s)
log10 (M)
0
0.2
0.4
5
10
15
20
25
30
35
40
45
-2
-4
-6
-8
-10
-12
-14

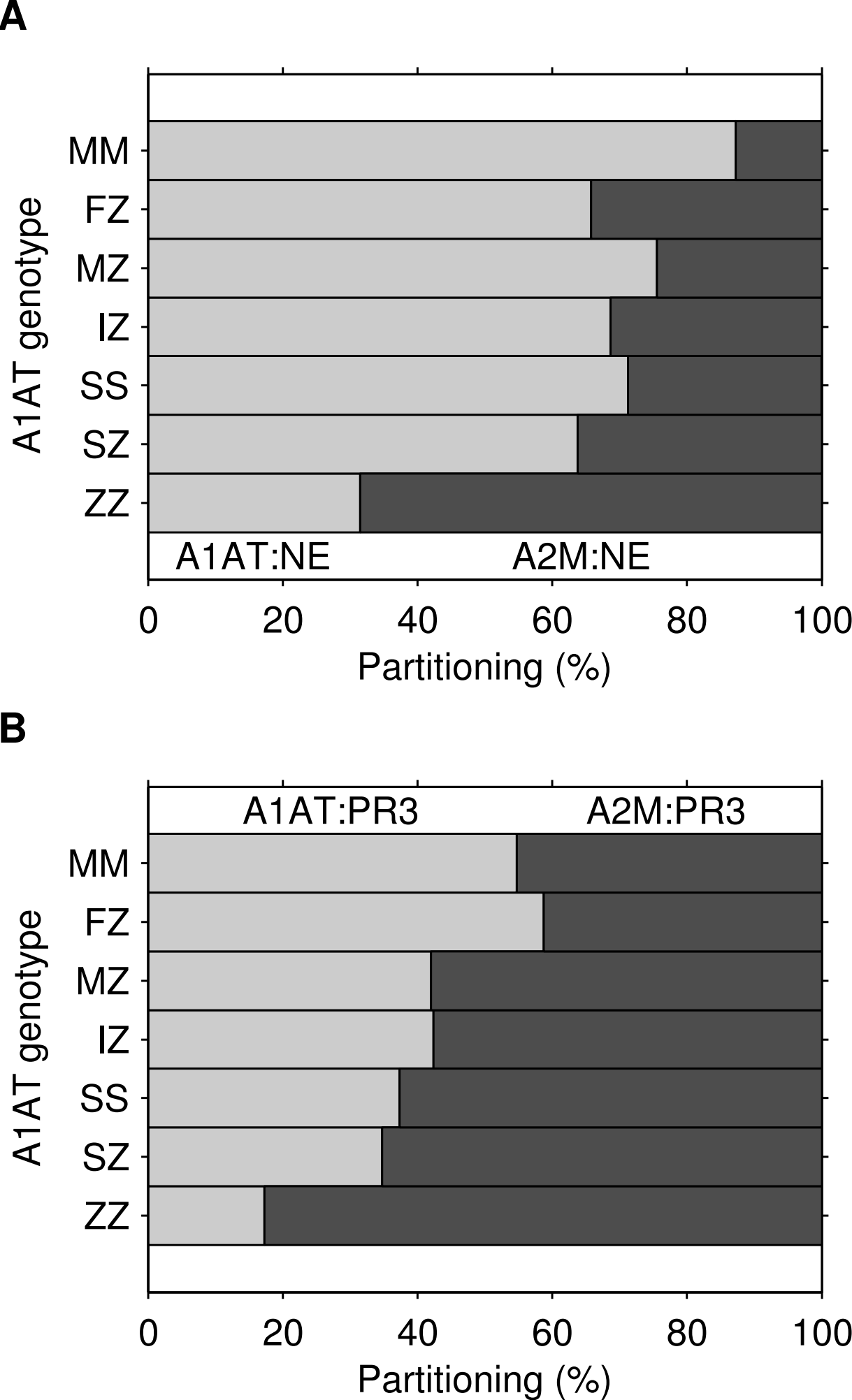
A
A1AT genotype
MM
FZ
MZ
IZ
SS
SZ
ZZ
A1AT:NE
A2M:NE
0
20
40
60
80
100
Partitioning (%)
B
A1AT:PR3
A2M:PR3
A1AT genotype
MM
FZ
MZ
IZ
SS
SZ
ZZ
0
20
40
60
80
100
Partitioning (%)